Direct measurement of barrier asymmetry in AlO_x/ZrO_y magnetic tunnel junctions using off-axis electron holography

Yu-Zi Liu,[1,*] W. G. Wang,[2,†] T. Moriyama,[2] John Q. Xiao,[2] and Z. Zhang[3]
[1]*Beijing National Laboratory for Condensed Matter Physics, Institute of Physics, Chinese Academy of Sciences, P.O. Box 603, Beijing 100080, China*
[2]*Department of Physics and Astronomy, University of Delaware, Newark, Delaware 19716, USA*
[3]*Beijing University of Technology, 100 Pingle Yuan, Chao Yang District, Beijing 100022, China*
(Received 21 November 2006; revised manuscript received 2 February 2007; published 24 April 2007)

Off-axis electron holography was used to investigate the barrier profile of the $Py/AlO_x/ZrO_y/Py$ magnetic tunnel junctions with different ZrO_y thicknesses. The tunneling magnetoresistance (TMR) has a strong dependence on bias voltage and the bias voltage for maximum TMR is shifted from zero. This shift increases with ZrO_y barrier thickness due to the increasing barrier asymmetry in the junctions. The evolution of barrier asymmetry was directly observed by the phase change of the off-axis electron holography, which unambiguously shows the barrier profile changes from triangular to trapezoidal shape as increasing of ZrO_y thickness.

DOI: 10.1103/PhysRevB.75.134420 PACS number(s): 73.40.Gk, 85.70.Kh, 61.14.Nm

I. INTRODUCTION

Magnetic tunnel junctions (MTJs) attract much attention for their fundamental physics and potential applications in high-density magnetic read head sensors and magnetic random access memories.[1] Recently, MTJs with very high TMR ratio were fabricated by Parkin,[2] Yuasa,[3] and other groups[4] using MgO as the barrier. It is expected the industrial products utilizing the high tunneling magnetoresistance will be available soon. However, there are still many issues that remain to be fully understood. One of them is the bias voltage dependence of TMR. In most cases, TMR decreases with increasing bias voltage and even changes to negative at higher bias voltage.[5] This behavior was explained by magnon excitation,[6] density of states,[7] impurity assisted tunneling,[8,9] and quantum coherence.[10] It is often found that the bias voltage for maximum TMR is shifted from zero when TMR's bias voltage dependence is asymmetric. It is advantageous for applications because we can engineer the MTJs to work at maximum TMR under a specific bias. The asymmetric bias dependence has been studied in MTJs with dissimilar electrodes, such as $Co/Al_2O_3/Py$ ($Py=Ni_{81}Fe_{19}$) junctions[11] and $Co/Al_2O_3/Co$ junctions with different crystal structures of Co.[12] It has also been studied in MTJs with the different barrier heights at the top and bottom interfaces as seen in a $Co/Cu/Co/Al_2O_3/Co$ junction where the steplike potential barrier was created by diffusing Cu into the Al_2O_3 interface[13] and in $FeCo/TaO_x/FeCo$ junctions where the asymmetric barrier was formed by different oxidation conditions.[14] Many techniques have been used to characterize the ultrathin barrier in MTJ.[14,15] As a direction characterization technique, transmission electron microscopy (TEM) has been widely used to determine the relationships between microstructures and physical properties.[16] Here it was used to investigate the barriers shape revolution with different Zr thickness.

In this paper, we report the fabrication and detection of the trapezoidal-like tunnel barrier formed by AlO_x/ZrO_y. It was found that the bias voltage dependence of TMR is clearly asymmetric and the degree of asymmetry increases as the ZrO_y layer gets thicker. The evolution of barrier asymmetry was directly observed by off-axis electron holography. As compared to the observation of barrier asymmetry using the photoconductance method by Koller *et al.*,[14] not only can off-axis electron holography detect barrier asymmetry directly, but it can also determine the barrier width accurately.

II. EXPERIMENTS

The MTJs were deposited by magnetron sputtering system with a base pressure of 2×10^{-7} Torr. The structure of the as-deposited film is $Si/Py(21)/Cu(6.5)/FeMn(12)/Py(6)/Al(0.45)+Zr(0-2.6)$ $+oxidation/Py(6)/Ta(5.4)$, where Py stands for $Ni_{81}Fe_{19}$, and the numbers in parentheses are layer thickness in nanometers. The barrier was fabricated by depositing a uniform 0.45-nm-thick Al layer and wedge-shaped Zr layer with thickness ranging from 0 to 2.6 nm, followed by plasma oxidation at 60 mTorr for 120 s. MTJ samples with areas from 0.0078 to 0.125 mm^2 were defined by standard photolithography and ion-beam etching processes. More detailed fabrication procedures can be found elsewhere.[17] The transport measurements were done using the four-probe method at room temperature. The positive bias voltage refers to current flowing from the top electrode to the bottom electrode. The specimens for transmission electron microscope (TEM) study were prepared by standard process. Special care was taken to ensure the thickness was uniform in the region interested. After the thickness of the cross-sectional sample is reduced to less than 10 μm by standard procedures, a 3° low angle Ar focused ion beam at 4 kV was applied to the sample for 3–5 min with the sample rotating in 360°. The focused ion beam was stopped when a hole appeared in the center of the specimen. Finally the thickness of the specimen was further reduced in the Fischione 1010 ion milling device with spread Ar ion beam. The ultramicrotome of *RMC Powertom XL* system was used to prepare the cross section ultrathin slice.

A Philips CM 200-FEG TEM with a field emission gun equipped with an electrostatic biprism inserted at the posi-

 ©2007 The American Physical Society

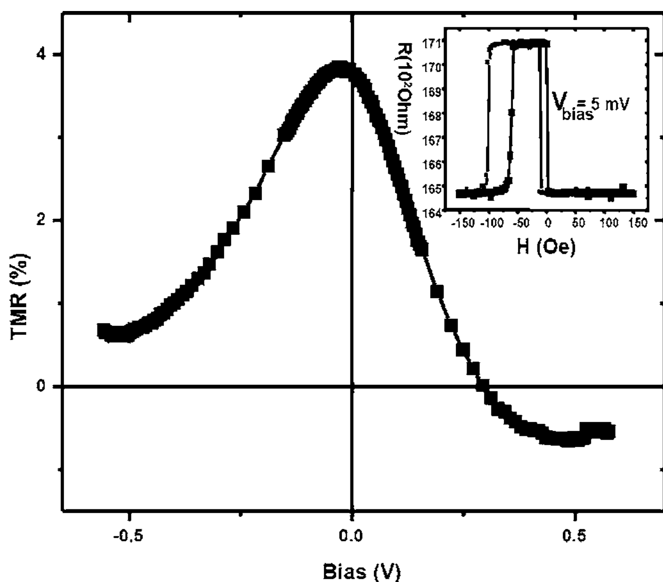

FIG. 1. A typical bias dependence of TMR in Si/Py(21)/Cu(6.5)/FeMn(12)/Py(6)/Al(0.45)+Zr(0–2.6) +oxidation/Py(6)/Ta(5.4) junction. The inset shows the *R-H* curve measured at 5 mV.

tion of the selected aperture holder was used to characterize the films' microstructure and to conduct the off-axis electron holography experiments. The off-axis electron holography was performed in high resolution transmission electron microscopy (HREM) mode by applying 120 V positive bias voltage to the electrostatic biprism. The holograms were processed using the Holoworks[18] package embedded in Digital Micrograph software. A TECNAI G^2 F20 with a field emission gun equipped with energy dispersive x-ray analysis (EDX) and high-angle annular dark-field (HAADF) devices was used to investigate the Al and Zr distribution.

III. RESULTS AND DISCUSSIONS

A. TMR bias voltage dependent measurements

A typical bias voltage dependence of the TMR is shown in Fig. 1. We denote the voltage where TMR has maximum as V_M. The asymmetric property of the TMR bias voltage dependence is clearly seen. The V_M shifts from zero about 25 mV for this particular junction, and we can see that the TMR dependence on positive and negative bias voltage is very different. The TMR rapidly reduces as the positive bias voltage increases and eventually changes to negative, but has a relatively weaker dependence with negative bias voltage and never changes sign even at large bias voltage. The origin of this shift of V_M is due to the asymmetry of the tunnel barrier. It is known the AlO_x has a higher barrier height (2.4 eV) (Ref. 7) than ZrO_y (1.6 eV).[19] When AlO_x was fabricated on the bottom electrode and ZrO_y was fabricated under the top electrode, an asymmetric composite barrier was formed. At zero bias voltage, the asymmetric barrier can be represented by a trapezoid with a relatively low average barrier height as Fig. 2(a). When a negative bias voltage is applied to the junction, the Fermi level of the top electrode is

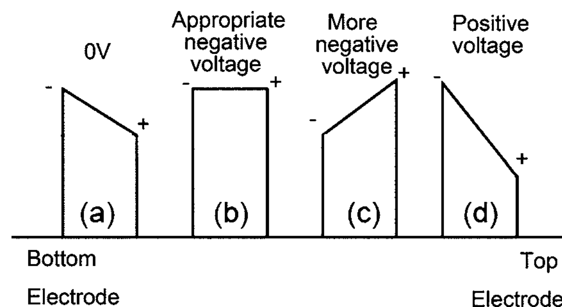

FIG. 2. The schematic diagram showing the expected changes in barrier shape with bias voltage change from zero to negative as (a), (b), and (c). (d) shows the barrier shape under positive bias voltage.

raised, changing the shape of the barrier towards a square potential as Fig. 2(b). At this bias voltage when the trapezoid-like barrier becomes rectangular, namely when the asymmetric barrier profile becomes symmetric, TMR reaches maximum. This is consistent with the fact that the maximum TMR is always observed when the barrier shape is symmetric.[7,14] However, if the applied negative bias voltage keeps increasing, the barrier will become asymmetric again as Fig. 2(c) and TMR will start to decrease. In contrast, when a positive bias voltage is applied, the Fermi level of the bottom electrode is going to be increased, which will make the barrier shape more asymmetric as Fig. 2(d) than the case of zero bias, so the TMR decreases monotonically.

The V_M of a series of junctions with different ZrO_y thickness was measured and summarized in Fig. 3. The V_M increases with the nominal Zr width increasing. It is natural to assume that there is a large degree of the mixing between Zr layer and Al layer at the thinner end of the Zr wedge, and more pure Zr exists at the top interface when Zr layer gets thicker, thus resulting in a more asymmetric barrier after oxidation. This increasing of barrier asymmetry was probed directly by the off-axis electron holography as shown next.

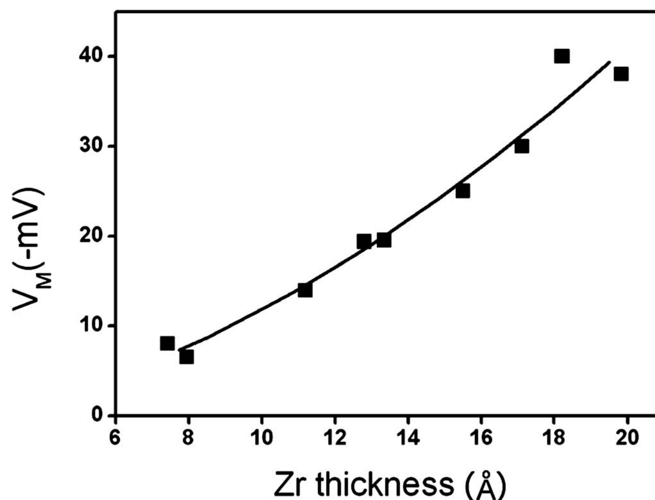

FIG. 3. The bias voltage at maximal TMR for a series of MTJs with different Zr thickness. The solid line is a guide for the eye only.

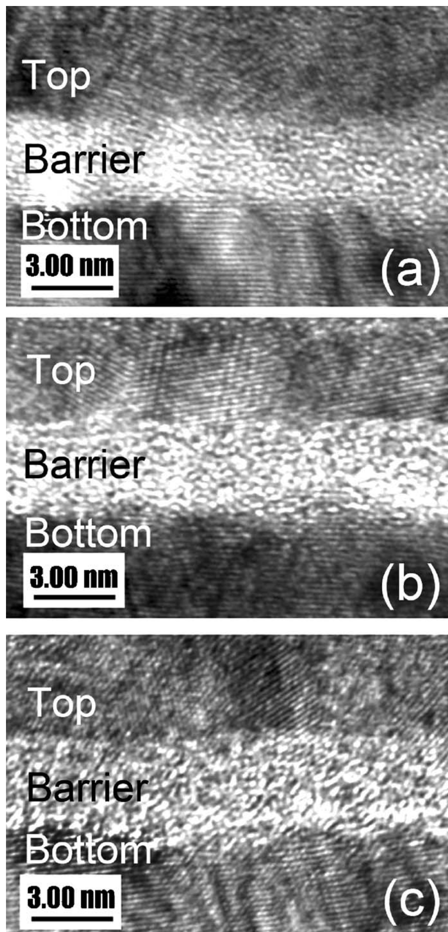

FIG. 4. The HREM cross-sectional images of MTJs with the 1.3-nm-thick Zr (a), 1.7-nm-thick Zr (b), and 1.9-nm-thick Zr (c). The top and bottom in (a) indicate the top electrode and bottom electrode, respectively.

B. TEM measurements

TEM studies were carried out to investigate the relation between the V_M and barrier asymmetry. Figures 4(a)–4(c) show the HREM images of the MTJs with the 1.3-, 1.7-, and 1.9-nm-thick Zr, respectively. For these specimens, the bottom and top electrodes all have very strong (111) texture, which is consistent with previous research.[15,16] The barrier widths of these three MTJs determined from the HREM images are about 3.05, 3.29, and 3.41 nm, respectively. HREM is a powerful tool to characterize the crystal material structure on the atomic scale, but not an ideal technique to investigate the amorphous barrier layers in these samples. Here, from the HREM we could not explain the V_M changing with the Zr thickness.

As shown in our previous publication,[16] off-axis electron holography is a very useful tool to study the amorphous barrier in MTJs by detecting the phase change in high resolution. Two electron waves traveling on both sides of the biprism were attracted towards the biprism by applying positive bias voltage. Higher bias voltage would induce a broader interference pattern and smaller fringe spacing. The phase change of the electron wave in TEM that has passed

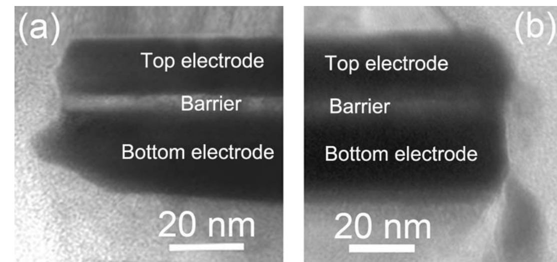

FIG. 5. The bright field images of the left side (a) and right side (b) of ultrathin slice, which was cross cut from a standard TEM specimen for electron holography. The preferential thinning can be seen directly.

through a material can be extracted from the hologram. It can be used to detect the inner potential and probe the barrier shape directly and determine the barrier width accurately. In our experiments there is no external electric field. The magnetic field influence can be neglected since the magnetic field of the electrode is far less than the magnetic field induced by the TEM column. Thus the phase change can be written as[20]

$$\varphi = C_E V_0(x,y) t(x,y),$$

where C_E is a constant dependent on the high voltage of TEM, in the case of an accelerating voltage of 200 kV in our experiments, C_E equals 7.3×10^{-3} rad V^{-1} nm^{-1}, $t(x,y)$ is the thickness of the specimen, and $V_0(x,y)$ is the mean inner potential of the material. It is critical to keep sample thickness uniform in the area of interest if we want to represent the barrier profile by φ. The preferential thinning in the barrier region during membrane preparation was minimized by using high quality Gatan PIPs focused ion beam in a very short time. It was confirmed by Fig. 5. The (a) and (b) images were taken from both sides of an ultrathin slice, which was cross cut from a standard TEM specimen for electron holography by ultramicrotome of *RMC Powertom XL* system. We can find that the preferential thinning exists among the top-bottom-electrodes and the barrier layer. However, almost no preferential thinning exists in the composite barrier. The thickness of the barrier layer formed by AlO_x and ZrO_y can be considered constant and the barrier profile can be represented by φ.

The standard hologram of the MTJ with 1.3-nm-thick Zr is shown in Fig. 6(a). For subsequent compensation of artifacts of the reconstructed phase image stemming from geometric distortions, a reference hologram was recorded as suggested in Ref. 21. For this reason, the specimen was retracted from the hologram very carefully to ensure that the optical parameters of the microscope did not change. The fringe spacing of hologram without specimen in the beam is about 0.15 nm. So the spatial resolution of the reconstructed phase image is about 0.3–0.45 nm because every detail resolved after reconstruction had to be sampled with 2–3 hologram fringes. The phase detection limit is about $\frac{2\pi}{50}$ which was estimated using $\sigma_\varphi = \sqrt{2/(V^2 N)}$[22] under the visibility V about 50% and electron dose N about 600. Here the signal transfer efficiency for CCD camera is set as 1. Figure 6(b) shows the phase image reconstructed from (a). The phase

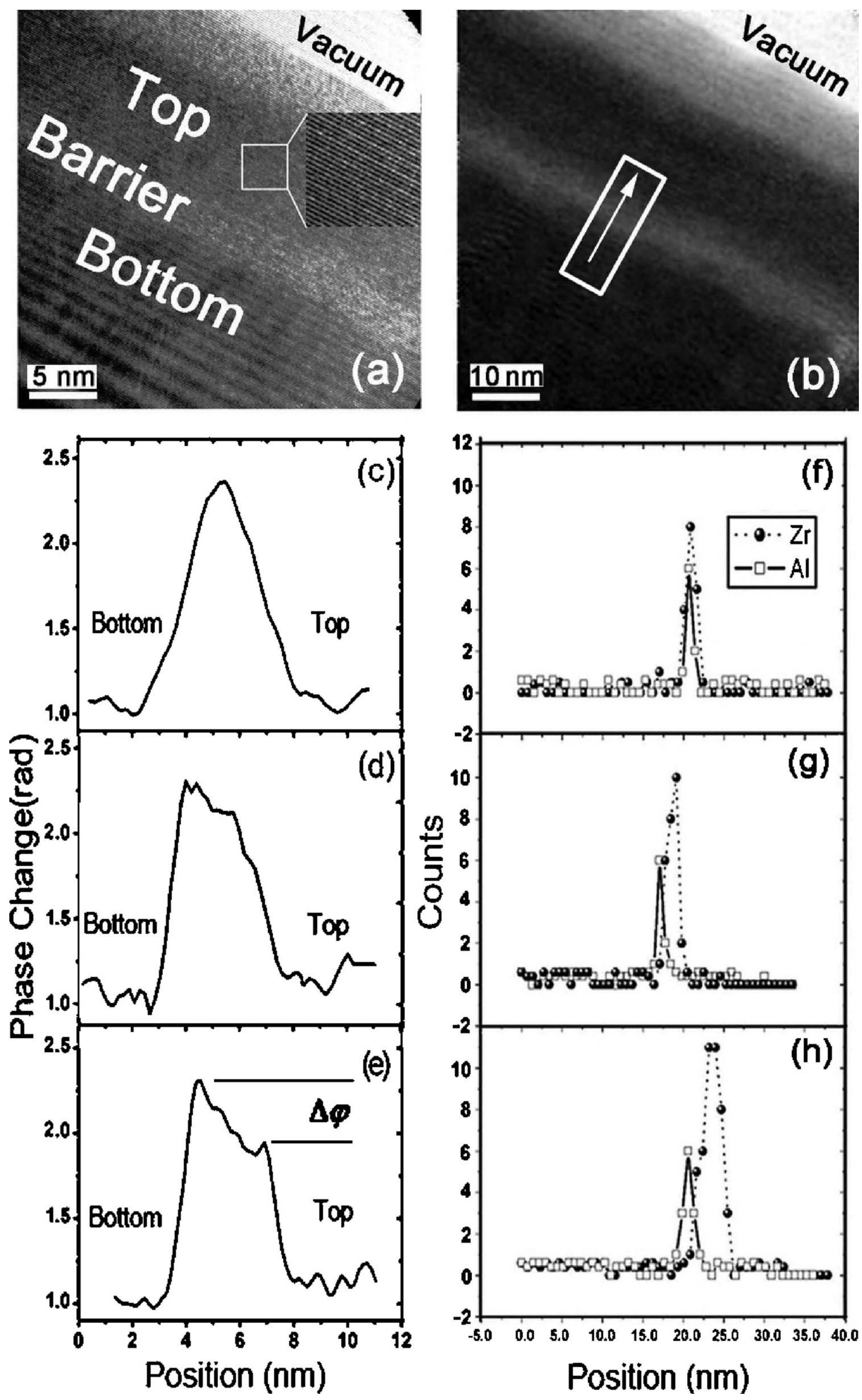

FIG. 6. (a) The standard hologram of MTJ with 1.3-nm-thick Zr. (b) is the reconstructed phase image of (a). (c), (d), (e) are the averaged phase profile for Zr thickness of 1.3, 1.7, and 1.9 nm, respectively. (f), (g), (h) Al and Zr distribution for (c), (d), and (e), respectively, from line scanning EDX.

change can be quantitatively displayed under averaging the phase image over 15 pixels perpendicular to the profile direction. The profile is perpendicular across the barrier. The arrow indicates the phase change scanning direction, from bottom electrode to top one. The averaged phase changes of the MTJs with 1.3-, 1.7-, and 1.9-nm-thick Zr are shown in Figs. 6(c)–6(e), respectively, with φ of the bottom electrode normalized for comparison. The barrier widths, 3.06, 3.27,

and 3.40 nm, of these three MTJs can be measured from the full-width at half-maximum of the phase change peaks. They are consistent with the width directly measured by HREM. φ is symmetric with a 1.3-nm-thick Zr layer as shown in Fig. 6(c). With the increase of Zr layer thickness to 1.7 and 1.9 nm, φ becomes more and more asymmetric as shown in Figs. 6(d) and 6(e). It is believed that this increasing degree of asymmetry in φ with Zr layer thickness is caused by the increasing asymmetry composition of the tunneling barrier. It is consistent with our expectation that there is a large degree of the mixing between the Zr and Al layers at the thinner end of the Zr wedge, and more pure Zr exists at the top interface when the Zr layer gets thicker, thus resulting in a more asymmetric barrier after oxidation.

C. Al and Zr distribution measurement

In order to clarify the degree of mixing for the AlO_x and ZrO_y layers, the EDX line scan analysis was carried out to study the distribution of Al and Zr across the barrier. The results are shown in Figs. 6(f)–6(h) corresponding to the samples shown in (c), (d), and (e), respectively. The line scan was done perpendicular to the barrier from bottom electrode to top electrode. It can be clearly seen that the distribution peaks of Al and Zr are gradually separated with increasing Zr thickness, giving more evidence for the formation of a more asymmetric barrier at the thicker end of the Zr wedge. The low record counts are caused by the small quantity of Al and Zr in the barrier and short time data collection to avoid the specimen holder fluctuation effect. From the results we can give a proposal that the barrier revolution is from homogeneous $AlZrO_x$ (mixed entirety) to AlO_x-$AlZrO_x$-ZrO_y (mixed partially) compositional barrier with Zr thickness increasing.

IV. CONCLUSION

In conclusion, we reported the direct measurement of barrier asymmetry in MTJs using off-axis electron holography. The bias voltage at maximum TMR in MTJs with AlO_x and ZrO_y composite barrier increases with Zr thickness due to an increase of barrier asymmetry. This evolution of barrier asymmetry was directly observed by phase change of electron holography. The barrier profile was found to change from triangular shape to trapezoidal shape as increasing of ZrO_y thickness.

ACKNOWLEDGMENTS

The authors would like to acknowledge Ministry of Science and Technology (Grant No. 2002CB613502) of China and NSF DMR Grant No. 0405-136.

*Electronic address: yzliu@blem.ac.cn
†Electronic address: weigang@UDel.edu

[1] J. S. Moodera and G. Mathon, J. Magn. Magn. Mater. **200**, 248 (1999).
[2] S. S. P. Parkin, C. Kaiser, A. Panchula, P. M. Rice, B. Hughes, M. Samant, and S. H. Yang, Nat. Mater. **3**, 862 (2004).
[3] S. Yuasa, T. Nagahama, A. Fukushima, Y. Suzuki, and K. Ando, Nat. Mater. **3**, 868 (2004).
[4] D. D. Djayaprawira, K. Tsunekawa, M. Nagai, H. Maehara, S. Yamagata, N. Watanabe, S. Yuasa, Y. Suzuki, and K. Ando, Appl. Phys. Lett. **86**, 092502 (2005).
[5] M. Sharma, S. X. Wang, and J. H. Nickel, Phys. Rev. Lett. **82**, 616 (1999).
[6] J. S. Bae, K. H. Shin, T. D. Lee, and H. M. Lee, Appl. Phys. Lett. **80**, 1168 (2002).
[7] X. H. Xiang, T. Zhu, J. Du, G. Landry, and J. Q. Xiao, Phys. Rev. B **66**, 174407 (2002).
[8] A. M. Bratkovsky, Phys. Rev. B **56**, 2344 (1997).
[9] E. Y. Tsymbal and D. G. Pettifor, J. Appl. Phys. **85**, 5801 (1999).
[10] F. F. Li, Z. Z. Li, M. W. Xiao, J. Du, W. Xu, and A. Hu, Phys. Rev. B **69** 054410 (2004).
[11] X. H. Xiang, T. Zhu, G. Landry, J. Du, Y. W. Zhao, and J. Q. Xiao, Appl. Phys. Lett. **83**, 2826 (2003).
[12] P. LeClair, J. T. Kohlhepp, C. H. van de Vin, H. Wieldraaijer, H. J. M. Swagten, W. J. M. de Jonge, A. H. Davis, J. M. MacLaren, J. S. Moodera, and R. Jansen, Phys. Rev. Lett. **88**, 107201 (2002).
[13] H. Bruckl, J. Schmalhorst, G. Reiss, G. Gieres, and J. Wecker, Appl. Phys. Lett. **78**, 1113 (2001).
[14] P. H. P. Koller, H. J. M. Swagten, W. J. M. de Jonge, H. Boeve, and R. Coehoorn, Appl. Phys. Lett. **84**, 4929 (2004).
[15] P. LeClair, H. J. M. Swagten, J. T. Kohlhepp, R. J. M. van de Veerdonk, and W. J. M. de Jonge, Phys. Rev. Lett. **84**, 2933 (2000).
[16] F. Shen, T. Zhu, X. H. Xiang, J. Q. Xiao, E. Voelkl, and Z. Zhang, Appl. Phys. Lett. **83**, 5482 (2003).
[17] T. Zhu, X. Xiang, F. Shen, Z. Zhang, G. Landry, D. V. Dimitrov, N. Garcia, and J. Q. Xiao, Phys. Rev. B **66**, 094423 (2002).
[18] E. Volkl, L. F. Allard, and B. Frost, J. Microsc. **180**, 39 (1995).
[19] J. G. Wang, P. P. Freitas, E. Snoeck, P. Wei, and J. C. Soares, Appl. Phys. Lett. **79**, 4387 (2001).
[20] E. Voelkl, L. Allard, and D. Joy, *Introduction to Electron Holography* (Plenum, New York, 1999).
[21] A. Tonomura, Adv. Phys. **41**, 59 (1992).
[22] A. Harscher and H. Lichte, Ultramicroscopy **64**, 57 (1996).